Energy Reports 8 (2022) 7751–7763

Contents lists available at ScienceDirect

Energy Reports

journal homepage: www.elsevier.com/locate/egyr

Are subsidies for thermally-driven solar-assisted cooling systems consistent? A critical investigation for Southern Italy

L. Marletta, G. Evola *, R. Arena, A. Gagliano

Università degli Studi di Catania, Viale A. Doria 6, 95125 Catania, Italy

ARTICLE INFO

Article history:
Received 10 January 2022
Received in revised form 1 June 2022
Accepted 6 June 2022
Available online xxxx

Keywords:
Solar cooling
Absorption chiller
Electric chiller
Hybrid cooler
Incentives

ABSTRACT

The growing availability of low-cost electricity-driven air-conditioning systems has determined a huge increase in the electricity demand for space cooling, especially in warm and hot climates. In this framework, thermally-driven solar-assisted cooling systems are a very interesting alternative, since they are mainly fed by converting the largely available solar radiation into thermal energy: however, their economic convenience is still questionable. For this reason, many EU states have introduced suitable subsidies: in Italy, the so-called "Conto Termico" proposes cash-back incentives proportional to the thermal energy delivered by the solar field.

This study investigates the suitability and consistency of these subsidies, by considering a case study including a thermally-driven solar-assisted absorption chiller that cools down an office building located in Palermo (Southern Italy). The study looks into the sizing of the system and evaluates its techno-economic feasibility by considering the incentives introduced by the Italian "Conto Termico". The results highlight that the proposed solar-assisted absorption cooling system can reduce primary energy demand and CO_2 emissions by around 75% if compared to a conventional electric chiller, under a reasonable sizing of the solar section. The subsidies are proportional to the thermal energy delivered by the solar collectors, and thus tend to favour the adoption of high collecting surfaces: for instance, installing 2 m^2 of evacuated tube solar collectors per unit cooling capacity ensures relatively low payback periods of 15 years or even less. However, the energy performance of the system does not improve accordingly with higher collecting surfaces, since a non-negligible rate of delivered thermal energy is wasted, as witnessed by the decreasing seasonal COP. Moreover, Flat Plate Collectors are improperly penalized, and the real local operating conditions are not considered in the calculation. This suggests that the rationale leading Italian subsidies are not consistent, and needs being improved.

1. Introduction

The growth of residential construction in emerging markets, but also the increased request of thermal comfort, has generated an impressive boost in air conditioning (AC) demand, as forecasted in recently published authoritative reports by DOE (Goetzler et al., 2016) and IEA (Anon, 2018) devoted to the "Future of air conditioning". According to these documents, the use of electric energy for space cooling has more than tripled between 1990 and 2016, and the sales of electric ACs have almost quadrupled. Currently about 1.6 billion AC units are in use, consuming almost 20% of the total energy use in buildings (Anon, 2018).

The rising demand of final energy for cooling purposes also entails strain on electricity distribution networks, with consequent occurrence of brownouts and/or blackouts over large territorial areas, thus creating enormous risks in terms of productivity and safety problems for the population. Moreover, conventional electricity-driven cooling systems imply pollutant emissions due to burning fossil fuels for electricity production, as well as other environmental issues associated with the Ozone Depletion Potential (ODP) and the Global Warming Potential (GWP) of the working fluids released to the environment at the end of life.

This critical scenario calls for new cooling technologies that are less prone to electricity and more environmentally friendly: for instance, suitable technologies can be driven by solar energy. Indeed, the so-called "Solar Cooling (SC)" or Solar Air Conditioning (SAC)" systems have a number of favourable issues. First of all, the direct use of solar energy as a driver, instead of the electricity taken from the distribution network, alleviates the intensity of electricity peaks. In addition, avoiding the use of conventional cooling machines prevents the environmental impact of refrigerants. Furthermore, SC makes cooling loads in phase with

* Corresponding author.
E-mail address: gevola@unict.it (G. Evola).

https://doi.org/10.1016/j.egyr.2022.06.010

Nomenclature

a_1	Linear loss coefficient (W/(m^2 K))
a_2	Quadratic loss coefficient (W/(m^2 K^2))
A_g	Gross collector area (m^2)
A_{sc}	Net solar collector area (m^2)
B_y	Annual economic subsidy (€/year)
C_1	Coefficient of valorization of the thermal energy (€/kWh)
c_p	Specific heat (J/(kg K))
E_{cool}	Electricity consumption of the hybrid cooler (kWh)
E_{pump}	Electricity consumption of the pump of the hybrid cooler (kWh)
E_{solar}	Electricity consumption of the pump in the solar circuit (kWh)
g	Solar transmission factor (–)
G_{min}	Minimum solar irradiance (W/m^2)
G_T	Solar irradiance on a tilted surface (W/m^2)
I_{CO2}	Emission Factor (g/kWh)
m	Mass flow rate (kg/s)
η_0	Optical efficiency of the collector (–)
η_{coll}	Thermal efficiency of the collector (–)
P_{aux}	Electric power consumed by the auxiliary equipment (kW)
P_{cool}	Nominal electric power absorbed by the hybrid cooler (kW)
P_{pump}	Electric power of the pump (kW)
Q_{aux}	Thermal energy supplied by the back-up boiler (kWh)
Q_c	Cooling power (kW)
Q_{coll}	Thermal power provided by solar collectors (kW)
Q_{ev}	Thermal power absorbed in the evaporator (kW)
Q_F	Cooling demand (kWh)
Q_{gen}	Thermal power supplied to the generator (kWh)
Q_{loss}	Heat losses from the tank (kWh)
$Q_{sol,u}$	Useable solar irradiation (kWh/m^2)
Q_{ST}	Thermal energy supplied to the solar tank (kWh)
Q_u	Energy collected by the solar field (kWh/m^2)
T_A	Heat rejection temperature (°C)
T_a	Ambient temperature (°C)
T_G	Heat supply temperature (°C)
T_{in}	Water temperature at the inlet (°C)
T_m	Mean temperature of the collecting surface (°C)
T_{out}	Water temperature at the outlet
τ_{pump}	Operating time of the pump (h)
U-value	Thermal transmittance (W/m^2 K)

Abbreviation

AC	Air conditioning
COP	Coefficient of Performance
DHW	Domestic hot water
DPT	Discounted Payback Time
ETC	Evacuated Tube Collectors
FPC	Flat Plate Collectors
GWP	Global Warming Potential
H2O-LiBr	Water – lithium bromide
H2O-LiCl	Water – lithium chloride
ODP	Ozone Depletion Potential
OSE	Overall System Efficiency
RES	Renewable Energy Sources
SAC	Solar Air Conditioning
SC	Solar Cooling
SCOP	Solar Coefficient of Performance
SF	Solar Fraction
SPT	Simple Payback Time

the source availability: indeed, in the summer cooling energy demand and solar energy availability are almost synchronized, with non-negligible relief in terms of thermal storage sizing.

Once solar energy is harvested, the cooling power can be achieved in a number of ways. Besides the electric chillers fed by PV modules, there are three different technologies, all mature and commercially available, based either on absorption/adsorption principle or on the use of desiccant materials, which give raise to thermally driven chillers as an alternative to electrically driven chillers (Hennings et al., 2013; Palomba et al., 2019). In solar-driven cooling systems, the driving thermal energy is partially collected through solar thermal technologies: in this case, the Solar Fraction (SF) is the fraction of driving thermal energy coming from the solar section. A relevant literature is available today concerning SC systems (Jakob, 2014; Gagliano et al., 2014; Buonomano et al., 2018; Pons et al., 2012) and a growing attention is being paid by the scientific community to this subject (Anon, 2012b, 2015). Namely several IEA tasks are devoted to SAC since Task 25 (1999-2004) and subsequent Tasks 38, 45, 48, 53, up to the last one, Task 65, currently in progress.

Amongst the above-mentioned SC technologies, thermally-driven absorption chillers are by far the most common ones. They exploit thermal energy to release vapour from a liquid working pair containing a highly volatile component; the vapour completes an inverse cycle and produces cooling at the evaporator, eventually being reabsorbed in liquid form in the absorber. The simplest absorption chiller is the single-effect type, but also available are the double and triple-effect chillers, where the heat rejected from the lower stages is transferred to the upper stages. Single-effect absorption chillers can be easily driven by Evacuated Tube Collectors (ETC) or common Flat Plate Collectors (FPC), as they need a driving temperature between 80 °C and 100 °C. Their Coefficient of Performance (COP), i.e. the ratio of the cooling capacity to the driving thermal power, ranges between 0.6 and 0.8 (Tawalbeh et al., 2020). In comparison to absorption chillers, adsorption chillers require even lower temperatures (50 °C – 80 °C), but their COP is lower (between 0.3 and 0.7). Moreover, their cost is considerably higher, which explains their low diffusion (Alahmer and Ajib, 2020).

In commercially available absorption chillers, the most frequently used working pairs are water–lithium bromide (H_2O-LiBr) and ammonia–water (NH_3-H_2O) (Sun et al., 2012). The success of H_2O-LiBr is due to the low boiling temperature and the high latent heat of water, the favourable operating pressures and the low toxicity. However, some limitations come from the risk of crystallization of the lithium bromide, the corrosiveness of the solution and the impossibility to achieve evaporation temperatures below 4 °C (Lahoud et al., 2021). Further working pairs like ammonia–sodium thiocyanate (NH_3-NaSCN), ammonia–calcium chloride (NH_3-$CaCl_2$) (Sarbu and Sebarchievici, 2015), ammonia–lithium nitrate (NH_3-$LiNO_3$) (Ayala et al., 1998), water – silica gel (H_2O-SiO_2) (Ul Qadir et al., 2020), and water–lithium chloride (H_2O-LiCl) (Bellos et al., 2016a), are not very competitive due to their modest performance. However, it was proven that H_2O-LiCl provides satisfying results if used in double stage absorption cycles (She et al., 2015). It is also important to remark that the great majority of the commercial water–lithium bromide absorption chillers are water cooled, meaning that they require the use of cooling towers to remove the absorption and condensation heat. The reason is that in these cooling devices the condenser temperature is usually beneath 35 °C, which makes heat rejection to outdoor air quite difficult, especially in the summer (Tawalbeh et al., 2020). However, a few air-cooled models are also available for regions with water scarcity (Monne et al., 2011). Coming to the cooling capacity, many single-stage absorption chillers have recently been developed in the small capacity range, identified by an upper threshold of 50 to 100 kW; several devices ranging from 4.5 to 20 kW are nowadays on the market (Altamirano et al., 2019).

Some studies highlighted that the SF in SC systems increases with the increase in the solar collector's field, as well as the size of the thermal storage needed to store solar energy when the cooling demand is low (Marcos et al., 2018; Pandya et al., 2017). Larger storage tanks commonly imply slower thermal discharge, slightly lower cold production but also higher Coefficient of Performance (COP) for the absorption chiller (Evola et al., 2013). However, the SF has an upper limit which determines an optimum solar collector area and an optimum volume of the thermal storage, above which only marginal improvements can be achieved.

In order to determine the sustainability of solar cooling systems, the financial convenience has also to be considered. Indeed, despite the rapid growth of the sector since its very beginning, the relatively high cost of the components in thermally-driven solar cooling systems has hindered to some extent their diffusion even in the Western countries. Currently, reliability and costs are maybe the most critical issues that make SC systems less convenient than traditional ones or other renewable-based cooling systems (Palomba et al., 2019; Otanicar et al., 2012). To correct this trend and enhance the use of Renewable Energy Sources (RES) also for cooling purposes, the EU has solicited the national communities to promote initiatives and offer incentives to solar cooling systems. For instance, in Italy – besides the encouraging feed-in tariffs reserved to PV systems – the SAC technologies (among others) are sustained by the so called "Conto Termico" (Anon, 2012a, 2016a), with cash-back incentives that are proportional to the thermal energy delivered by the solar field.

Despite the key role of financial issues to promote a wider adoption of solar-assisted cooling systems, only few studies have deepened this topic. For instance, Vasta et al. (2015) investigated the energy and financial performance of several SC systems in three different Italian cities by means of TRNSYS simulations, and demonstrated that "Conto Termico" can reduce the Discounted Payback Time (DPT) from around 34 years to 13–15 years. Instead, the payback time for a 70-kW solar-driven absorption chiller system, used in a hospital in Greece, was 11.6 years without funding and around 6 years with 40% funding on the initial costs (Tsoutsos et al., 2010). Bellos et al. presented an exergy, energy and financial evaluation of a solar-driven single-stage H_2O-LiBr absorption cooling system with driving temperatures between 100 °C and 135 °C (Bellos et al., 2016b): the results suggest that parabolic trough collectors optimize the thermal performance, but ETC allow the best financial performance. Finally, Figaj and Żołądek (2021) found out that – in a residential application – solar-assisted absorption cooling system with ETC ensure a Simple Payback Time (SPT) between 20 and 27 years, while slightly lower values are found in case of FPC. In this framework, the present paper further contributes to the knowledge of the financial and environmental performance of small-capacity solar-driven H_2O-LiBr absorption cooling systems. The investigation refers to a 35 kW water-cooled absorption chiller providing cooling to an office building, and considers several different values of the solar collecting surface. In order to assess the financial feasibility, the paper compares the proposed solar cooling system to a conventional cooling system based on an air-cooled vapour compression electric chiller, the latter being the most common and straightforward solution currently adopted for space cooling.

Unlike other recent studies that have investigated the optimization of financial and energy performance of absorption cooling chillers, based on complex dynamic simulations (Altun and Kilic, 2020; Asadi et al., 2018), the present paper relies on a simplified quasi-stationary monthly analysis. Indeed, the paper has the main scope of casting light on the effectiveness of the current incentive scheme for solar-assisted systems, while also providing a simplified tool for preliminary investigations in this direction.

The outcomes, expressed in terms of non-renewable primary energy savings, avoided CO_2 emissions, overall installation costs and payback time, point out that the incentives provided by "Conto Termico" are still essential to foster the adoption of solar-assisted absorption cooling systems in Italy. However, the current scheme shows a series of criticalities which should be tackled in order to promote the actual installation of efficient systems: indeed, incentives do not take into account the real local operating conditions, which may induce to oversize the solar field for the sake of profit, but without real benefits in terms of energy and environmental performance. The discussion of the results highlights possible improvements to the incentive scheme, and may be useful for governments and local authorities to promote solar cooling technologies coherently with their actual benefits in terms of environmental burden and management of energy resources.

2. Methodology

2.1. Solar cooling system

The schematic diagram of the solar cooling system under investigation is shown in Fig. 1. Here, the solar subsystem includes the collector field, a thermally insulated hot storage tank, an auxiliary boiler and the piping. Here, a gas-fuelled back-up boiler is preferred to an electric one, which would imply far higher primary energy demand.

The cooling subsystem integrates an absorption chiller, a hybrid cooler, and three pumps connected respectively to the generator, the evaporator and the heat rejection section of the absorption chiller. The hot water collected by the solar field might obviously be used also to provide space heating and domestic hot water (DHW), but this study is only concerned with the cooling purposes.

2.2. Energy balance in the solar collectors

The useful thermal power provided by the solar collectors and transferred to the storage tank is given by:

$$Q_{coll} = \dot{m} \cdot c_p \cdot (T_{out} - T_{in}) = \eta_{coll} \cdot A_{SC} \cdot G_T \quad (1)$$

Here, G_T is the solar irradiance on the unit tilted surface, A_{SC} is the net solar collector surface and η_{coll} is the thermal collector

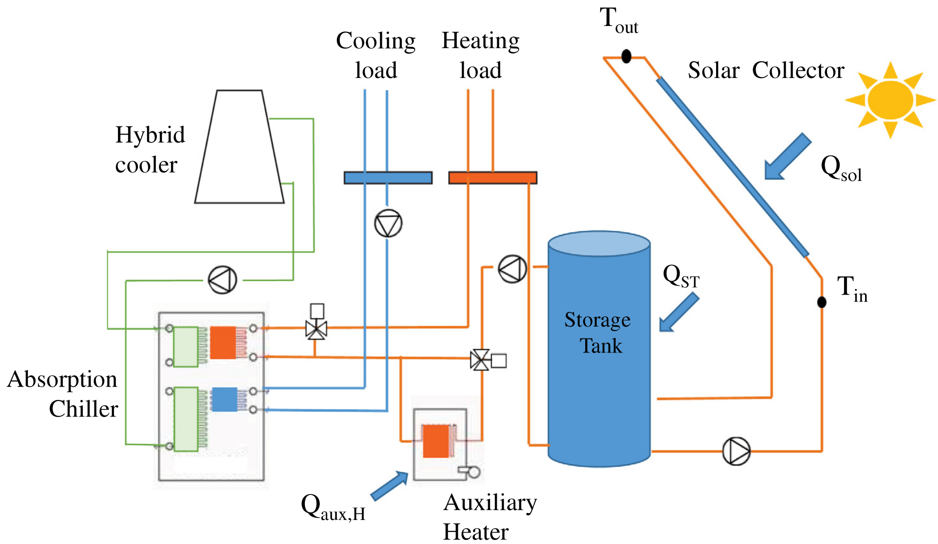

Fig. 1. General scheme of the solar-assisted cooling system.

efficiency, calculated according to the EN Standard 12975 (Anon, 2010) as:

$$\eta_{coll} = \eta_0 - a_1 \cdot \frac{(T_m - T_a)}{G_T} - a_2 \cdot \frac{(T_m - T_a)^2}{G_T} \tag{2}$$

In Eq. (2) η_0, a_1 and a_2 are the optical efficiency of the collector, the linear loss coefficient and the quadratic loss coefficient, respectively. T_a is the ambient temperature and T_m the mean temperature of the collecting surface calculated as the mean between the inlet (T_{in}) and the outlet (T_{out}) water temperatures.

2.3. Solar storage tank

The storage tank volume must not be excessive, in order to contain heat losses, increase the mean operating temperature and reduce the total cost. According to Henning (Henning, 2007), the size of the storage tank (expressed in litres) should be around 50 times the collector surface (in m^2) for common consumption profiles; this is the value retained in this paper. The heat losses from the tank to the environment (Q_{loss}) are usually quantified through a heatlosscoefficient, whose typical value for well-insulated tanks is 0.5 W m^{-2} K^{-1}. In this study, for the sake of simplification heat losses are approximated to 10% of the thermal energy delivered by the solar field, including also the heat losses in the primary solar circuit.

2.4. Absorption chiller modelling

Water–LiBr absorption chillers are used for air conditioning applications operating with evaporating temperatures above 0 °C. Their Coefficient of Performance (COP) is the ratio of the thermal power absorbed in the evaporator and causing the cooling effect (Q_{ev}), to the thermal power supplied to the generator (Q_{gen}) plus the electric power consumed by the internal auxiliaryequipment (P_{aux}).

$$COP = \frac{Q_{ev}}{Q_{gen} + P_{aux}} \tag{3}$$

It is well known that the COP of an absorption system gets higher as the supply temperature increases and/or the ambient temperature (air or water) for heat rejection decreases. Here, constant heat supply temperature is assumed, thus it is reasonable to keep a constant COP in the calculations.

2.5. Cooling device

The thermal power that the absorption chiller rejects to the environment is:

$$Q_c = Q_{gen} + Q_{ev} \tag{4}$$

In a water-cooled absorption chiller, heat rejection can be performed by means of cooling towers, dry coolers or hybrid coolers. Hybrid coolers combine dry and evaporative cooling: indeed, they operate similarly to dry cooling systems in the winter, while in the summer running water evaporates in suitable pre-cooling pads and cools the air down to the adiabatic saturation condition (Anon, 2021a), and thus below the ambient temperature. In this study, since the weather conditions refer to a warm climate, the adoption of a hybrid cooler is necessary to perform effective heat rejection.

However, both dry and hybrid coolers are affected by non-negligible electricity consumption due to the fans. For instance, the power absorption considered in this study is 2.25 kW: this value refers to a commercial product whose rejection capacity is compatible with the capacity of the selected absorption chiller (Anon, 2021a). Further details are provided in Section 3.3.

2.6. Overall performance parameters

The performance of a solar cooling system over a certain period of time can be assessed through the so-called *Solar Fraction* (SF), defined as the ratio of the harvested solar energy to the overall thermal energy needed to feed the absorption chiller over that period. The latter term is equivalent to the amount of energy transferred from the solar field to the solar tank (Q_{ST}) plus the contribution of the back-up boiler ($Q_{aux,H}$). In formula (Rodriguez-Aumente et al., 2012; Kalogirou, 2014):

$$SF = \frac{Q_{ST}}{Q_{ST} + Q_{aux,H}} \tag{5}$$

$$Q_{ST} = \left(Q_{sol,u} \cdot \eta_{coll} \cdot A_{SC}\right) - Q_{loss} = 0.9 \cdot Q_{sol,u} \cdot \eta_{coll} \cdot A_{SC} \tag{6}$$

In Eq. (6), for the sake of simplification, heat losses in the solar section are approximated to 10% of the solar thermal production, which justifies the multiplier in the right-end side of the equation (0.9). The useable solar irradiation ($Q_{sol,u}$) is calculated through the *utilizability method*, which includes only those operating conditions that make it possible to reach sufficiently high temperatures in the solar field. This approach identifies the minimum solar irradiance (G_{min}) that allows at least balancing the heat losses from the solar field (Oliveti and Arcuri, 1996): in this condition, the circulation pump in the primary solar circuit should only work if $G_T > G_{min}$, where G_{min} can be retrieved from Eq. (2) under the constraints $\eta_{coll} = 0$ and $a_1 >> a_2$.

$$G_{min} \simeq \frac{a_1 \cdot (T_m - T_a)}{\eta_0} \tag{7}$$

Finally, the solar coefficient of performance (SCOP) for the solar cooling system is given by Eq. (8) (Lizarte et al., 2012):

$$SCOP = \frac{Q_{ST} \cdot COP}{A_{SC} \cdot G_T} \tag{8}$$

2.7. Solar-assisted cooling system: performance analysis

In this study, the performance of the solar-assisted cooling system is assessed through the simplified semi-stationary procedure outlined in the Italian Standard UNI/TS 11300-1:2014 (Anon, 2014).

For every month, starting with the hourly solar irradiance $G_{T,h}$ that can be retrieved from the PVGIS website (Anon, 2021b), but considering only those values that exceed the lower threshold stated in Eq. (7), it is possible to calculate the monthly useful solar irradiation $Q_{sol,u,i}$ as follows:

$$Q_{sol,u,i} = \sum_{day} \sum_{h} G_{T,h} \qquad \text{if } G_{T,h} > G_{min,i} \tag{9}$$

Then, the monthly value of the thermal energy collected in the storage can be determined from Eq. (6). The thermal energy needed by the chiller for the given month "i" can be computed from the monthly cooling demand $Q_{F,i}$ and the COP of the absorption chiller:

$$Q_{gen,i} = \frac{Q_{F,i}}{COP} \tag{10}$$

Finally, the monthly thermal energy provided by the auxiliary system $Q_{aux,i}$ is:

$$Q_{aux,i} = Q_{gen,i} - Q_{ST,i} \tag{11}$$

The monthly solar coefficient of performance SCOP (also called OSE: Overall System Efficiency) for the whole solar cooling plant is finally determined by Eq. (8). All results are reported in terms of average daily values.

2.8. Cost analysis

The overall installation costs are obtained by summing up the costs for all the system's components, i.e. the absorption chiller, the solar collectors, the back-up boiler, the hybrid cooler and the storage tank, whose size is proportional to the net collecting surface. However, the investment can be regarded as the difference between the installation costs of the solar-assisted system and the traditional cooling system.

The annual cash flow generated by installing the solar-assisted cooling system corresponds to the difference between the energy bills of the traditional cooling system and the solar-assisted one: to this aim, the costs of the energy vectors are assumed as 0.25 €/kWh for electricity and 0.7 €/m^3 for natural gas. Finally, the Simple Payback Time (SPT) is the ratio of the initial investment by the annual cash flow. Here, all those installation costs that are common to both types of cooling systems – such as the fan-coils, the distribution network from the chiller to the fan-coils, the pump and the control unit, the cold storage tank – are not included in the comparison because they do not impact on the calculation of the SPT.

Obviously, the solar cooling system has much higher initial costs than a traditional vapour compression electric chiller: therefore, making the transition to this technology convenient also from an economic point of view means resorting to state incentives, namely the "Conto Termico" (Anon, 2016a) in Italy. In this case, the annual economic subsidies are calculated by Eq. (12):

$$B_Y = C_1 \cdot A_g \cdot Q_u \qquad (€/\text{year}) \tag{12}$$

Here A_g is the gross area of the collectors installed, and C_1 is the *coefficient of valorization* of the thermal energy, whose values allowed by "Conto Termico" for solar cooling systems are summarized in Table 1.

Instead, the term Q_u is the annual thermal energy collected by the solar field (in kWh per unit gross collector area), referred to the locality of Würzburg: this is 333 kWh/m^2 for the selected Evacuated Tube Collectors when operating with a mean fluid temperature equal to 75 °C, as certified in the technical sheets. Please consider that if $A_g \leq 50$ m^2 the incentive is paid for only two years, while above this threshold it is paid for five years.

Finally, one must remark that the costs for electricity and fuel in Italy show non-negligible fluctuations with time, and change according to the regional area: in the authors' opinion, the proposed values are a good estimation of the average price in the second semester of 2021. However, in order to account for their possible variation and the consequent impact on the results, the study includes a sensitivity analysis that considers a variation by 20% starting from the proposed values.

3. Case study and design parameters

3.1. Description of the building

The building here considered is an office building located in Palermo, Italy (Lat. 38°6′43″, Long. 13°20′11″). Fig. 2 shows the monthly average values for the daily horizontal solar irradiation and the outdoor air temperature in this city, and compares them with the values referring to Würzburg (Lat. 49° 46′ 59″, Long 9° 55′ 59), in Germany (Anon, 2021b). In fact, Würzburg is commonly used as a reference location for certifying the performance of the solar collectors, and even the Italian "Conto Termico" refers to it in the calculation of the subsides for solar thermal systems. This is quite unusual and unfair, since Palermo shows much more favourable weather conditions, which should be duly recognized by the incentive scheme. Indeed, in Würzburg the annual horizontal solar irradiation is almost 1100 kWh/m^2, while in Palermo this is 1690 kWh/m^2. Furthermore, the average outdoor air temperature in the summer months ranges between 22 °C and 25 °C in Palermo, while it lies between 16 °C and 20 °C in Würzburg.

The building has three floors and a rectangular plan along the East-West direction, with south facing glazed surfaces. The base closure is formed by a 260 mm floor slab, a 50 mm thick insulating board of polyurethane and a 50 mm thick concrete and cement mortar undercoat that supports the 10 mm ceramic tile cladding. The side walls are 300 mm thick and are formed from the inside by 10 mm inner plaster, a 200 mm lightened concrete board, a 70 mm fibreglass insulation panel and a further 20 mm outer plaster layer. The horizontal roof is made with a 15 mm interior plaster, a 180 mm floor slab, a 100 mm insulation layer, a 5 mm waterproofing layer covered with pebbles and stones. As for the transparent envelope, the fixtures are obtained with hardwood frames and low-emissivity double-glazing (4-12-4) filled with Argon. The solar transmission factor is g =

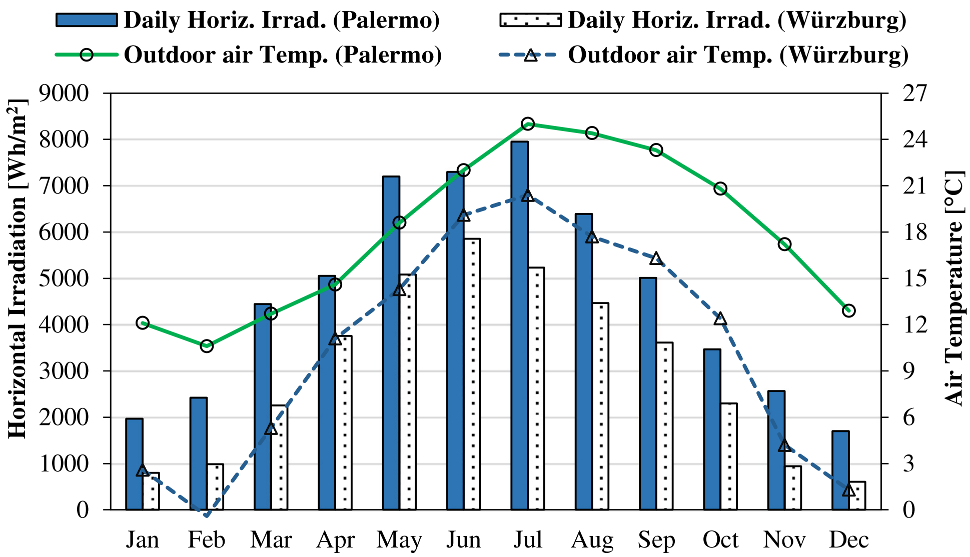

Fig. 2. Average monthly weather data for Palermo (Italy) and Würzburg (Germany).

Table 1
Coefficient of valorization for the thermal energy (C_1) Anon (2016a).

Gross collector area	$A_g \leq 12$ m^2	12 m$^2 < A_g \leq 50$ m^2	50 m$^2 < A_g \leq 200$ m^2
C_1[€/kWh]	0.43	0.39	0.13

Table 2
Geometric features of the selected building.

Number of floors	3
Net height of floors	3 m
Total external dispersing surface	914 m^2
Opaque external dispersing surface	792 m^2
Transparent external dispersing surface	122 m^2
Transparent to opaque ratio	0.15
Heated gross volume	4208 m^3
Shape Factor	0.217 m^{-1}
Net Floor Area	1453 m^2

Table 3
Thermal transmittance of the building components.

Component	U-value
Roof	0.298 W/m^2 K
Walls	0.437 W/m^2 K
Windows	1.972 W/m^2 K
Floor	0.365 W/m^2 K

0.67, as suggested for double glazing by the UNI/TS Standard 11300-1:2014 (Anon, 2014).

The relevant building data are collected in Table 2, while the thermal transmittance values of the building components, calculated according to EN UNI 6946 (Anon, 2017a), are shown in Table 2.

The internal loads are due to occupants, electronic devices and artificial lighting systems (see Table 3). Electronic devices are considered as low-density sources, equal to 20 W/m^2, while lighting is ensured by fluorescent lamps, whose design power absorption is set to 12 W/m^2. The air change rate is 0.5 vol/h for every room, except for kitchen and bathroom where it is 1.5 vol/h. The monthly cooling demand, based on semi-stationary energy balances as set in the UNI/TS Standard 11300-1:2014 (Anon, 2014) and by considering monthly average weather data, is mainly due to the internal loads, since the contribution of solar gains is mitigated by the presence of mobile shading devices, while the envelope has good insulation levels. The resulting average daily cooling demand in the summer months is reported in Table 4: these values result from dividing the monthly cooling demand by the number of days. The peak cooling load, occurring in July, is 36 kW.

3.2. water–lithium bromide absorption chiller

The nominal cooling capacity of the absorption chiller must match the building peak cooling load calculated in the previous section. In this application, the selected absorption chiller is Yazaki WFC SC 10, working with the water–lithium bromide pair. The chilled, cooling and hot water temperature can vary from 5.5 °C to 15.5 °C, 27 °C to 32 °C and 70 °C to 95 °C, respectively. Table 5 provides the main performance data of the absorption chiller in nominal conditions. In this study, the operating conditions slightly differ from nominal conditions, since the chiller operates with heat supply temperature T_G = 80 °C and heat rejection temperature T_A = 27 °C: however, the manufacturer also provides the curves for evaluating the performance as a function of these temperatures, and the resulting COP is 0.7

3.3. Hybrid cooler

The chosen model is Eurochiler ADcooler 80, whose technical specifications are summarized in Table 6. This hybrid cooler ensures the disposal of the correct amount of heat during the cooling period: indeed, it is able to reject a maximum of 82 kW,

Table 4
Average daily cooling demand in the summer.

	June	July	August	September
Cooling demand [kWh/d]	109.2	256.6	225.1	68.1

Table 5
Technical specifications of the selected absorption chiller Anon (2022).

Section	Parameter	Value
Chilled water	Cooling capacity	35 kW
	Water flow rate	1.52 L/s
	Temperatures	Inlet: 12.5 °C, Outlet: 7.5 °C
Cooling water	Heat rejection rate	85 kW
	Water flow rate	5.11 L/s
	Temperatures	Inlet: 29 °C, Outlet: 34 °C
Heating medium	Thermal power	50 kW
	Water flow rate	2.4 L/s
	Temperatures	Inlet: 85 °C, Outlet: 80 °C

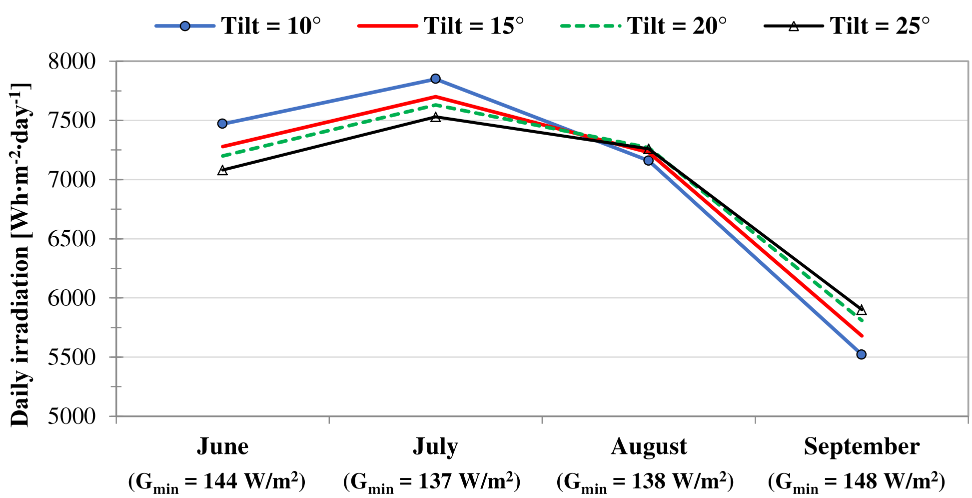

Fig. 3. Average useful daily irradiation values calculated with the utilizability method.

Table 6
Technical specifications of the hybrid cooler (Anon, 2021a).

Nominal cooling capacity	82 kW
Water flow rate	10.3 m^3/h
Pressure drop	15 kPa
Air flow rate	26,000 m^3/h
Absorbed electric power	2.25 kW

which is compliant with the heat rejection rate of the absorption chiller (see Table 5). The calculation of the energy consumption must also include the circulation pump in the cooling circuit: starting from the cooling water flow rate reported in Table 5, this has been estimated as $P_{pump} = 100$ W.

3.4. Solar field

As far as the solar field is concerned, the average value of the specific collector area for an absorption chiller is usually set between 2 and 2.5 m^2 per kW of cooling power (Anon, 2005, 2020). In this study, four different collecting surfaces of the solar field are investigated, namely 25, 35, 50 and 75 m^2, which correspond to a gross area of 41, 58, 83 and 124 m^2, respectively. The selected solar collector is the Evacuated Tube Collector Viessman Vitosol 200-TM, whose features are summarized in Table 7: as one can observe, in this type of collectors the gross area is 65% higher than the net collecting surface, and this is a very important detail, since the cash-back incentives ensured by "Conto Termico" depend on the gross area, which in fact largely overestimates the real collecting surface. In this study, we assume that the outlet water temperature form the solar collector is 85 °C.

4. Results

4.1. The exploitation of the solar resource

The available solar energy in the months of interest has been initially evaluated for several tilt angles of the solar collectors (10°, 15°, 20° and 25°), by considering south oriented surfaces. In addition, according to the utilizability method they are purified of that rate of solar radiation hitting the panel, but not sufficiently high to bring the hot water to the design temperature for the tank, set at 80 °C. The corresponding average monthly values for G_{min} (calculated through Eq. (7)) and the average daily useful solar irradiation are summarized in Fig. 3.

The selected tilt angle is 10°, since this allows to collect the highest average solar irradiation (7000 Wh/m^2 per day) and, in particular, the maximum irradiation in June and July, but also values not too far from the maximum in August. In September, this tilt angle is slightly penalizing, but still acceptable due to the lower cooling needs.

Fig. 4 shows the useful thermal energy delivered from the solar field and stored into the storage tank, which of course depends on the surface of solar collectors: here, four different possible values are considered. Then, starting from the daily cooling demand Q_F reported in Table 4, the thermal energy required as an input

Table 7
Technical specifications of Viessman Vitosol 200-TM.

η_o	a_1 [W/(m^2 K)]	a_2 [W/(m^2 K^2)]	Gross area [m^2]	Net collecting area [m^2]	Gross/net surface Ratio [–]
0.739	1.74	0.004	2.69	1.63	1.65

Table 8
Thermal input to the generator (Q_{gen}) and energy provided by the back-up (Q_{aux}).

	June		July		August		September	
A_{SC}[m^2]	Q_{gen} [kWh/d]	Q_{aux} [kWh/d]	Q_{gen} [kWh/d]	Q_{aux} [kWh/d]	Q_{gen} [kWh/d]	Q_{aux} [kWh/d]	Q_{gen} [kWh/d]	Q_{aux} [kWh/d]
25		43		247		214		18
35	156	0	367	200	322	171	97	0
50		0		128		106		0
75		0		8		0		0

Table 9
Solar Fraction and SCOP: monthly values.

A_{SC}	Solar Fraction (SF)					SCOP
	June	July	August	Sept.	Seasonal	
25 m^2	0.72 (–)	0.33 (–)	0.34 (–)	0.82 (–)	0.45	0.41
35 m^2	1.00 (+0.01)	0.46 (–)	0.47 (–)	1.00 (+0.14)	0.61	0.40
50 m^2	1.00 (+0.44)	0.65 (–)	0.67 (–)	1.00 (+0.63)	0.75	0.35
75 m^2	1.00 (+1.17)	0.98 (–)	1.00 (+0.01)	1.00 (+1.45)	0.99	0.31

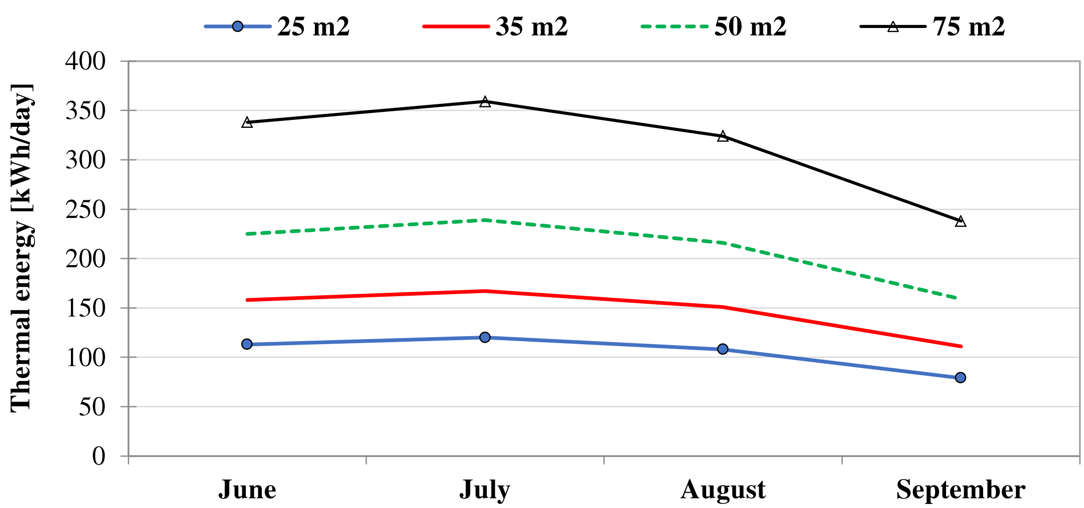

Fig. 4. Thermal energy produced by the solar system — daily values (Q_{ST}).

to the chiller is calculated by Eq. (10), and the auxiliary thermal energy Q_{aux} with Eq. (11). The results are reported in Table 8.

Furthermore, the SF achieved in each month, the seasonal SF and the SCOP are calculated and reported in Table 9. The values within brackets indicate the rate of thermal energy from the solar field exceeding what is strictly necessary to feed the absorption chiller: this proves that the solar section is oversized. As one can observe, by installing just 25 m^2 of solar collectors, the SF exceeds 70% in September and June, while in July and August only 33%–34% of the thermal energy required by the absorption chiller is covered by solar energy. For a larger solar field (35 m^2), which corresponds to 1.0 m^2 per kW of installed cooling power, almost half of the needs are supplied in July and August. Instead, when A_{SC} = 50 m^2, solar energy would cover about 65%–67% of the needs in July and August, but there would be an excess of thermal production in June (+44%) and September (+63%).

Finally, assuming that A_{SC} = 75 m^2, the cooling demand is covered almost entirely even in the hottest months, but this obviously leads to significant overproduction in June (+ 117%) and September (+ 145%), which might be used for other purposes (e.g. domestic hot water). The overproduction is also highlighted by the SCOP: indeed, this decreases with the increase in the installed area. It is interesting to observe that a strong correlation holds between the values reported in Table 8 and those in Table 9.

4.2. Energy comparison with a conventional cooling system

The overall energy performance of the solar cooling system was then assessed and compared with that of a traditional system, namely an air-cooled vapour-compression electric chiller, with a nominal cooling power of 36 kW and an average COP = 3. The monthly electricity consumption of the conventional chiller is estimated just by dividing the monthly cooling demand by the average COP value.

For the sake of comparison, the electricity consumption in the absorption cooling system is also needed. This is given by the hybrid cooler (E_{cool}) and its circulation pump (E_{pump}), plus the circulation pump in the solar circuit (E_{solar}) and the absorption chiller itself; however, the electricity consumption of the absorption chiller can be neglected. More in detail, E_{cool} and

Table 10
Comparison of the annual electricity consumption.

Net collector area [m^2]	25	35	50	75
Solar cooling system [kWh]	1502	1538	1592	1682
Electric chiller [kWh]	6589			

Table 11
Monthly and annual consumption of natural gas in the back-up of the SC system.

A_{SC} [m^2]	June [m^3]	July [m^3]	August [m^3]	September [m^3]	Total [m^3]
25	145	826	714	60	1745
35	0	666	570	0	1236
50	0	426	353	0	779
75	0	26	0	0	26

E_{pump} are calculated by multiplying their nominal power by the equivalent full load hours of operation; this leads to Eq. (13), where $P_{cool} = 2.25$ kW and $P_{pump} = 0.1$ kW are the nominal electric power absorbed by the hybrid cooler and its circulation pump, respectively, while 82 kW is the nominal heat rejection rate.

$$E_{el} = \left(E_{cool} + E_{pump}\right) + E_{solar} = \left[\underbrace{\frac{Q_{gen} + Q_{ev}}{82}}_{\text{Equivalent full load hours of operation}} \cdot \left(P_{cool} + P_{pump}\right)\right] + \underbrace{(50 + 5 \cdot A_{SC})}_{\text{Nominal electric power(solar pump)}} \cdot \tau_{pump} \tag{13}$$

Eq. (13) also includes the electricity demand for the circulation pump in the solar field: this is calculated according to the Italian UNI/TS Standard 11300-4 (Anon, 2016b) as a function of the net solar collector area, with $\tau_{pump} = 720$ h being the estimated total operating time (corresponding to 6 h per day on average). The results are resumed in Table 10.

Since the solar cooling system also needs a gas-fuelled back-up boiler, Table 11 reports the consumption of natural gas associated with the back-up boiler (see Table 8), based on a Lower Heating Value of 9.97 kWh/m^3 and a boiler efficiency of 0.90.

In order to calculate the non-renewable primary energy consumption associated with the electricity needs, these must be multiplied by 1.95: this is the factor adopted in Italy to convert final electricity demand into non-renewable primary energy, including the average efficiency for the production and distribution of electric energy to the end users. Moreover, one of the essential commitments of solar cooling systems is to reduce the use of non-solar energy sources, which gives rise to a reduction of CO_2 emissions. Hence, through the emission factors (I_{CO2}) associated with electricity (483 g/kWh) (Anon, 2017b) and natural gas (220 g/kWh), the amount of CO_2 released into the atmosphere has been calculated.

Fig. 5 shows the calculated primary energy values, while Table 12 summarizes the results in terms of CO_2 emissions.

If looking at both non-renewable primary energy demand and carbon dioxide emissions, more than 35 m^2 of solar collectors are required to make the solar cooling system less harmful to the environment than a traditional air-cooled electric chiller. Indeed, when $A_{SC} = 25$ m^2 the primary energy demand increases by 58% compared with a traditional electric chiller, while $A_{SC} = 50$ m^2 already ensures a reduction by 15%, which reaches 73% when $A_{SC} = 75$ m^2. A further environmental benefit associated with the absorption chiller is the avoidance of refrigerants with high Global Warming Potential, which is the case of many vapour compression chillers.

4.3. Economic analysis: the effectiveness of "conto termico"

The economic analysis starts with the assessment of the installation costs: the cost of the main system components is reported in Table 13, according to information provided by the manufacturers. The overall initial costs for the solar cooling system are reported in Table 14.

The cost comparison is summarized in Tables 15 and 16. In Table 15, one can observe that the percentage of the initial costs covered by the incentives in the Solar Cooling system increases with the collecting surface, and ranges from 30% ($A_{SC} = 25$ m^2) to 47% ($A_{SC} = 75$ m^2). This might suggest that a further increase in the collecting surface would be beneficial, but this option was not considered in this study because $A_{SC} = 75$ m^2 already ensures a very high Solar Fraction and a considerable excess of available thermal energy. In Table 16, the extra cost is the difference between the initial cost of the Solar Cooling system after applying the subsidies and that of the electric chiller. With a net collecting surface $A_{SC} = 35$ m^2 the extra cost is 16078 €; this would be recovered in 40 years thanks to almost 400 €/year of savings in the operating costs. It is necessary to install $A_{SC} = 75$ m^2 to get a more attractive payback time; in this case, the additional cost would be recovered in less than 16 years.

4.4. Costs of mitigating greenhouse gas emissions

In order to assess whether the attribution of the incentive complies with the actual environmental benefit, measured by the avoided CO_2 emissions, one can relate the increase in the allowed subsidy to the increased reduction of carbon dioxide emissions. To this aim, Table 17 shows the subsidies received as a function of the solar field area, the avoided CO_2 emissions over the entire operating life of the system (here assumed as twenty years) and their marginal unit cost in comparison with a baseline case, where $A_{SC} = 25$ m^2.

The results show that for a given increase in the collector area ($\Delta A_g = 25$ m^2), in the framework of the Italian incentive scheme, the benefit paid per unit mass of avoided CO_2 emissions still depends upon the installed collector area, and increases with it.

This cannot be justified on a rational basis, and in turn entails the risk of encouraging the sizing of the solar field beyond the techno-economic feasibility for the sake of profit. Indeed, any solar heat harvested in excess with respect to the actual thermal load results in an under-utilization of the solar collector area: this must be avoided, but the rationale of the incentives seems not to take it into proper account.

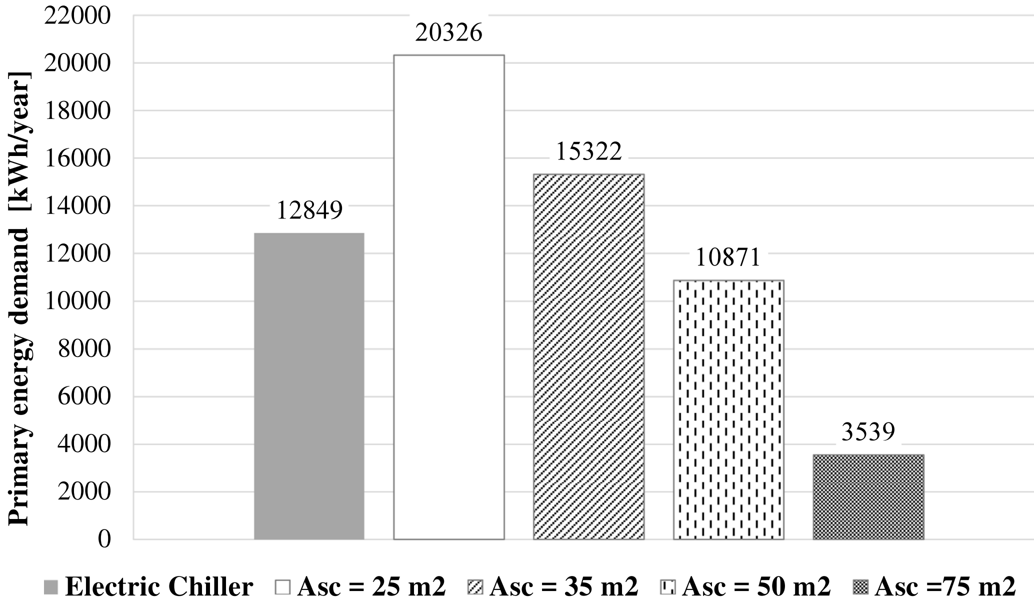

Fig. 5. Annual non-renewable primary energy demand for the proposed cooling systems.

Table 12
Annual CO_2 emissions associated with the proposed cooling systems.

Net collector area [m^2]		25	35	50	75
Solar Cooling system [kg/y]	Electricity	725	743	769	813
	Natural gas	3827	2711	1709	57
	TOTAL	4552	3454	2478	870
Electric chiller [kg/y]	3183				

Table 13
Installation costs for the different devices (the cost items with an asterisk include piping and circulation pump).

Electrical Chiller		11200	€
Absorption Chiller (Yazaki WFC SC 10)		19000	€
ETC Solar Panels (Viessman Vitosol 200-TM)*		390	€/m^2
Back-up Boiler (50 kW)*		1580	€
Hybrid Cooler (Eurochiler ADcooler 80)*		3250	€
Storage Tank(50 L/m^2)	1250 L (A_{SC} = 25 m^2)	1700	€
	1750 L (A_{SC} = 35 m^2)	2300	€
	2500 L (A_{SC} = 50 m^2)	3110	€
	3750 L (A_{SC} = 75 m^2)	4000	€

Table 14
Total installation costs for the solar cooling system.

Net collector area	25 m^2	35 m^2	50 m^2	75 m^2
Initial cost [€]	35280	39780	46440	57080

Table 15
Summary of costs and subsidies.

		Traditional plant	Solar cooling			
	Net collecting surface [m^2]	–	25	35	50	75
	Gross collecting surface [m^2]	–	41	58	83	124
	Installation costs [€]	11200	35280	39780	46440	57080
	Total Subsidies [€]	–	10716 (30.4%)	12502 (31.4%)	17860 (38.5%)	26791 (46.9%)
Operating Costs	Natural gas [€/y]	–	1221.5	865.2	545.3	18.2
	Electricity [€/y]	1647.0	375.5	384.5	398.0	420.5
	TOTAL [€/y]	1647.0	1597.0	1249.7	943.3	438.7

5. Discussion

The results presented in the above section strongly depend on the installation costs of the various system components, as well as on the price of the energy vectors, which however are rather variable. For this reason, the payback time has been calculated as a function of possible variations in the unit price of natural gas and electric energy, as well as in the overall initial cost of the solar cooling system.

Table 16
Economic comparison between traditional and Solar Cooling system.

A_{SC} [m^2]	SC installation cost applying incentives [€]	Extra-cost [€]	Savings on operating costs [€]	SPT [years]
25	24564	13364 €	–	–
35	27278	16078 €	397.6	40.4
50	28580	17380 €	703.9	24.7
75	30290	19090 €	1208.6	15.8

Table 17
Cost for CO_2 reduction considering the incentive.

A_{SC} [m^2]	Subsidies [€]	Increase of subsidies [€]	Total avoided CO_2 emissions [kg]	Marginal cost for avoided CO_2 emissions [c€/kg]
25	10716	–	–	–
35	12502	1786	21981.0	12.3
50	17860	7144	41507.1	17.2
75	26791	16075	73670.3	21.8

Table 18
Sensitivity of the simple payback time to the variation in some relevant prices.

Net collector area: $A_{SC} = 50$ m^2			
Variation in:	Gas price	Electricity price	SC installation costs
−20%	21.4 years	38.3 years	11.5 years
–	24.7 years	24.7 years	24.7 years
20%	29.2 years	18.2 years	37.8 years
Net collector area: $A_{SC} = 75$ m^2			
Variation in:	Gas price	Electricity price	SC installation costs
−20%	15.8 years	19.8 years	6.4 years
–	15.8 years	15.8 years	15.8 years
20%	15.8 years	13.1 years	25.2 years

The results of this sensitivity analysis are reported in Table 18. The financial performance of the SC system, under the current Italian incentive scheme, is of course strongly influenced by the initial installation costs: a reduction by 20% might ensure SPT = 11.5 years or even SPT = 6.4 years, respectively with $A_{SC} = 50$ m^2 and $A_{SC} = 75$ m^2. The sensitivity to the gas price is relatively low: lower gas prices would in principle favour the SC system, but such effect vanishes with a high collecting surface, since this minimizes the amount of natural gas consumed by the back-up boiler.

On the contrary, lower electricity prices would make thermally-driven solar cooling systems less convenient and almost unsustainable, even with the subsidies. These results are consistent with those reported by Huang and Zheng in 2018 (Huang and Zheng, 2018): their sensitivity analysis of a well-sized 35 kW solar-assisted thermally-driven absorption systems showed that the payback time ranges around 20 years, but only if subsidies are available in the same measure as those already allowed to PV systems. However, solar-assisted electricity-driven conventional chillers are much more convenient: thanks to the relatively low prices of the PV technology, their payback time is only around 7 years.

The results presented in this paper have also highlighted a series of inconsistencies in the incentive scheme. First, subsidies are proportional to the gross collector area, while the thermal energy delivered by the solar field depends on the net collector area. This approach favours the Evacuated Tube Collectors, where the ratio of the gross to the net area is high (1.65 for the model considered in this study), while it penalizes Flat Plate Collectors, whose gross area is very close to the net one. However, FPC still ensure good thermal efficiency in hot and sunny climates like in Palermo, especially in case of summer seasonal applications, and should not be penalized a priori.

A further inconsistency is that the subsidies are proportional to the solar energy harvested in a reference location (Würzburg, in Germany), which is commonly used for certifying the performance of the solar collectors. However, Palermo (and Southern Europe in general) has much more favourable weather conditions than Würzburg: in particular, the annual horizontal solar irradiation is almost 1100 kWh/m^2 in Würzburg, while in Palermo this is 1690 kWh/m^2. If one also considers the outdoor air temperature in Palermo (around 5 °C higher than in Würzburg, on average), this suggests that, if the subsidies were based on the actual thermal energy yield of the solar collectors operating in Palermo, they would roughly increase by 50%, with a consequent strong reduction in the payback period, leading to values below 10 years already with $A_{SC} = 50$ m^2.

The incentive scheme is inconsistent also because it encourages a large collecting surface, which would result in wasting solar thermal energy, with reductions in CO_2 that are not proportional to the increase in the subsidy. The remedy could be a corrective incentive scheme looking at the marginal cost for avoided CO_2 emissions: this means that the incentive should not be a function of the area of installed solar collectors, but of the avoided CO_2 emissions.

In light of the inconsistencies mentioned above, the following recommendations can be done regarding the annual economic subsidies (B_Y), currently calculated through Eq. (12):

- replacing the installed gross collector area (A_g) with the net collector area (A_{sc}), thus favouring solar collectors that optimize the occupied area for a given thermal yield;
- referring the annual thermal energy collected by the solar field (Q_u) to the specific climatic conditions of the selected site, instead of referring it to Würzburg. This would favour the use of solar-assisted cooling systems in those locations with higher solar irradiation;

Table 19
Proposed piecewise linear function to determine the coefficient of valorization C_1.

Solar Fraction	$0 < SF \leq 0.5$	$0.5 < SF \leq 0.75$	$0.75 < SF \leq 0.90$	$SF > 0.90$
C_1 [€/kWh]	from 0.13 to 0.39	from 0.39 to 0.43	from 0.43 to 0.13	from 0.43 to 0.13

- modifying the computation of the coefficient C_1, which currently depends on the gross collecting area (see Table 1), and make it dependant on the seasonal Solar Fraction (SF), for instance through a piecewise linear function where, as long as $SF \leq 0.75$, the unit incentive is higher, while for SF > 0.75 the incentive is reduced as the risk of oversizing may occur. No incentives should be given to the collecting area that implies SF > 0.90. A proposal for this scheme is reported in Table 19: here, the same values as the unit incentives as in the "Conto Termico" are used, but they are distributed according to the proposed approach, which would promote correctly sized solar plants.

Finally, the authors recognize that the model used for the performance analysis is a simplified one, since it operates on average daily energy balances (quasi-stationary approach) and is not based on dynamic hourly simulations. However, the aim of the paper is not a very detailed energy analysis, but rather highlighting possible inconsistencies in the incentive scheme. In this respect, a simplified methodology like the one here proposed may allow to rapidly compare different design solutions. The procedure can be extended to other solar thermally driven systems (e.g. based on adsorption chillers) with different size and location, by modifying the COP of the thermally driven chiller and the requested driving/rejection temperatures, as well as the weather data of the site of operation.

6. Conclusions

This paper investigates the effectiveness and consistency of the incentive scheme available in Italy for solar-assisted thermally-driven cooling systems. To this aim, the authors consider a case study including a small-capacity (35.2 kW) water–lithium bromide absorption chiller, used to cool an office building located in Palermo (Southern Italy). The performance of the solar cooling system, in terms of non-renewable primary energy consumption and CO_2 emissions, is assessed through a simplified semi-stationary approach with monthly energy balances. The analyses are carried out by varying the net area of the solar field between 25 m^2 and 75 m^2.

The results highlight that the proposed solar-assisted cooling system can reduce the primary energy demand by around 70% if compared to a conventional traditional electric chiller, if 2 m^2 of net collector area per kW cooling load are installed. Moreover, more than 35 m^2 of solar collectors (i.e. at least 1 m^2 per kW peak cooling load) are needed to make the solar cooling system more performing than a traditional electric chiller, even looking at CO_2 emissions. Further environmental benefit from the avoidance of refrigerants with high Global Warming Potential, such as those used in many vapour compression chillers.

For each configuration of the system, the techno-economic feasibility has been investigated in the framework of the subsidies introduced by the Italian law "Conto Termico". The outcome is that the investment costs are still quite high if compared to traditional vapour compression electric chillers: in order to reduce the payback time to a reasonable value (SPT = 15.8 years), large solar collector surfaces are needed, since the subsidies are proportional to the size of the solar field.

However, several inconsistencies emerge in the incentive scheme. Indeed, the subsidies are proportional to the gross collector area, while the actual harvested solar energy depends on the net collector area; moreover, the subsidies do not consider the real operating conditions, but those of a reference location (Würzburg, Germany) with obvious consequences in the profitability of the solar plant. Finally, the findings reveal that the benefit paid per unit avoided CO_2 emission increases with the installed collector area: this suggests that the incentive rationale may favour oversized solar systems, without real benefits in terms of energy environmental performance, not to say about a misuse of those public resources purposely aimed at reducing the environmental burden.

CRediT authorship contribution statement

L. Marletta: Conceptualization, Formal analysis, Writing – review & editing. **G. Evola:** Conceptualization, Methodology, Formal analysis, Writing – original draft, Writing – review & editing. **R. Arena:** Investigation, Data analysis, Visualization, Writing – original draft. **A. Gagliano:** Conceptualization, Methodology, Data analysis, Supervision, Writing – original draft, Writing – review & editing.

Declaration of competing interest

The authors declare that they have no known competing financial interests or personal relationships that could have appeared to influence the work reported in this paper.

Data availability

Data will be made available on request.

References

Alahmer, A., Ajib, S., 2020. Solar cooling technologies: state of the art and perspectives. Energy Convers. Manage. 214, 112896.
Altamirano, A., Le Pierrès, N., Stutz, B., 2019. Review of small-capacity single-stage continuous absorption systems operating on binary working fluids for cooling: theoretical, experimental and commercial cycles. Int. J. Refrig. 106, 350–373.
Altun, A.F., Kilic, M., 2020. Economic feasibility analysis with the parametric dynamic simulation of a single effect solar absorption cooling system for various climatic regions in Turkey. Renew. Energy 152, 75–93.
Anon, 2005. Deutsche gesellshaft fur sonnenenergie. Planning and Installing Solar Thermal Systems: A Guide for Installers. Architects and Engineers; Earthscan, London, UK.
Anon, 2010. EN 12975-1:2006 A1:2010. Thermal solar systems and components - Solar collectors - Part 1: General Requirements.
Anon, 2012a. DM 28/12/2012 Incentivazione della produzione di energia termica da fonti rinnovabili di piccole dimensioni, GU (1) del 2/1/2013 (in Italian).
Anon, 2012b. Solar heating and cooling. In: Technology Roadmap. IEA Publications.
Anon, 2014. UNI/T.S. 11300-1:2014 Prestazioni energetiche degli edifici - Parte 1: Determinazione del fabbisogno di energia termica dell'edificio per la climatizzazione estiva ed invernali (in Italian).
Anon, 2015. Solar Heating and Cooling for Residential Applications. IEA-ETSAP and IRENA, Technology Brief R12.
Anon, 2016. DM 16/02/2016: Aggiornamento della disciplina per l'incentivazione di interventi di piccole dimensioni e la produzione di energia termica da fonti rinnovabili, GU (51) del 2/3/2016 (in Italian).
Anon, 2016. UNI/TS 11300-4:2016, Parte 4: Utilizzo di energie rinnovabili e di altri metodi di generazione per la climatizzazione invernale e per la produzione di acqua calda sanitaria (in Italian).
Anon, 2017. EN UNI 6946:2017, Building components and building elements — Thermal resistance and thermal transmittance — Calculation methods.
Anon, 2017. Technical annex to the SEAP template instructions document: The Emission Factors-Covenant of Mayors.

Anon, 2018. The future of cooling. Opportunities for Energy-Efficient Air-Conditioning. IEA Publications.
Anon, 2020. National Agency for the Development of Renewable Energy and Energy Efficiency (ADEREE).
Anon, 2021. https://pdf.directindustry.com/pdf/eurochiller/adcooler/20502-228757.html.
Anon, 2021. https://ec.europa.eu/jrc/en/pvgis.
Anon, 2022. Yazaky specifications. Available at: https://yazaki-nordic.se/onewebmedia/FT_WFC_SC_SH_10_en.pdf. (Accessed 06 April 2022).
Asadi, J., Amani, P., Amani, M., Kasaeian, A., Bahiraei, M., 2018. Thermo-economic analysis and multi-objective optimization of absorption cooling system driven by various solar collector. Energy Conv. Manag. 173, 715–727.
Ayala, R., Heard, C.L., Holl, F.A., 1998. Ammonia/lithium nitrate absorption/compression refrigeration cycle, part II. experimental. Appl. Therm. Eng. 18, 661–670.
Bellos, E., Tzivanidis, C., Antonopoulos, K.A., 2016a. Exergetic and energetic comparison of LiCl-H2O and LiBr-H2O working pairs in a solar absorption cooling system. Energy Convers. Manage. 123, 453–461.
Bellos, E., Tzivanidis, C., Antonopoulos, K.A., 2016b. Exergetic, energetic and financial evaluation of a solar driven absorption cooling system with various collector types. Appl. Therm. Eng. 102, 749–759.
Buonomano, A., Calise, F., Palombo, A., 2018. Solar heating and cooling systems by absorption and adsorption chillers driven by stationary and concentrating photovoltaic/thermal solar collectors: modelling and simulation. Renew. Sustain. Energy Rev. 82, 1874–1908.
Evola, G., Le Pierrès, N., Boudehenn, F., Papillon, P., 2013. Proposal and validation of a model for the dynamic simulation of a solar-assisted single-stage LiBr/water absorption chiller. Int. J. Refrig. 36, 1015–1028.
Figaj, R., Żołądek, M., 2021. Experimental and numerical analysis of hybrid solar heating and cooling system for a residential user. Renew. Energy 172, 955–967.
Gagliano, A., Patania, F., Nocera, F., Galesi, A., 2014. Performance assessment of a solar assisted desiccant cooling system. Therm. Sci. 18 (2), 563–576.
Goetzler, W., Guerney, M., et al., 2016. The future of air conditioning for buildings. U.S.-DOE.
Henning, H.M., 2007. Solar assisted air conditioning of buildings - an overview. Appl. Therm. Eng. 27 (10), 1734–1749.
Hennings, H.M., Motta, M., Mugnier, D., 2013. Solar cooling handbook. In: A Guide to Solar Assisted Cooling and Dehumidification Processes. Ambra Verlaag.
Huang, L., Zheng, R., 2018. Energy and economic performance of solar cooling systems in the hot-summer and cold-winter zone. Buildings (8), 37.
Jakob, U., 2014. Technologies and perspectives of solar cooling systems. In: AHK Conference Solar Thermal World, Sydney.
Kalogirou, S., 2014. Designing and Modeling Solar Energy Systems in Solar Energy Engineering, second ed. Academic Press.
Lahoud, C., El Brouche, M., Lahoud, C., Hmadi, M., 2021. A review of single-effect solar absorption chillers and its perspective on lebanese case. Energy Rep. 7, 12–22.
Lizarte, R., Izquerdo, M., Marcos, J.D., Palacios, E., 2012. An innovative solar-driven directly air-cooled LiBr-H2O absorption chiller prototype for residential use. Energ. Build. 47, 1–11.
Marcos, J.D., Lizarte, R., Varela, F., Palacios-Lorenzo, M.E., Blanco-Marigorta, A.M., 2018. A solar air-cooled high efficiency absorption system in dry hot climates, reduction of water consumption and environmental impact. Therm. Sci. 22 (5), 2151–2162.
Monne, C., Alonso, S., Palicin, F., Serra, L., 2011. Monitoring and simulation of an existing solar powered absorption cooling system in Zaragoza (Spain). Appl. Therm. Eng. 31, 28–35.
Oliveti, G., Arcuri, N., 1996. Solar radiation utilisability method in heat pipe panels. Sol. Energy 57 (5), 345–360.
Otanicar, T., Taylor, R.A., Phelan, P.E., 2012. Prospects for solar cooling – An economic and environmental assessment. Sol. Energy 86, 1287–1299.
Palomba, V., Wittstadt, U., Bonanno, A., Tanne, N., Harborth, N., Vasta, S., 2019. Components and design guidelines for solar cooling systems: The experience of ZEOSOL. Renew. Energy 141, 678–692.
Pandya, B., Patel, J., Mudgal, A., 2017. Thermodynamic evaluation of generator temperature in LiBr-water absorption system for optimal performance. Energy Procedia 109, 270–278.
Pons, M., Anies, G., Boudehenn, F., Bourdoukan, P., Castaing-Lasvignottes, J., Evola, G., Le Denn, A., Le Pierrès, N., Marc, O., Mazet, N., Stitou, D., Lucas, F., 2012. Performance comparison of six solar-powered air-conditioners operated in five places. Energy 46, 471–483.
Rodriguez-Aumente, P.A., Lecuona, A., Legr, M., Ventas, R., 2012. Domestic hot water consumptions vs solar thermal energy storage: The optimum size of the storage tank. Appl. Energy 97, 897–906.
Sarbu, I., Sebarchievici, C., 2015. General review of solar-powered closed sorption refrigeration systems. Energy Convers. Manage. 105, 403–422.
She, X., Yin, Y., Xu, M., Zhang, X., 2015. A novel low-grade heat-driven absorption refrigeration system with LiCl–H_2O and LiBr–H_2O working pairs. Int. J. Refrig. 58, 219–234.
Sun, J., Fu, L., Zhang, S., 2012. Review of working fluids of absorption cycles. Renew. Sustain. Energy Rev. 16, 1899–1906.
Tawalbeh, M., Salameh, T., Albawab, M., Al-Othman, A., M., El Haj Assad, Alami, A.H., 2020. Study of a single effect lithium bromide-water absorption chiller powered by a renewable heat source. J. Sustain. Dev. Energy Water Environ. Syst. 8 (3), 464–475.
Tsoutsos, T., Aloumpi, E., Gkouskos, Z., Karagiorgas, M., 2010. Design of a solar absorption cooling system in a Greek hospital. Energy Build. 42, 265–272.
Ul Qadir, N., Said, S.A.M., Mansour, R.B., Imran, H., Khan, M., 2020. Performance comparison of a two-bed solar-driven adsorption chiller with optimal fixed and adaptive cycle times using a silica gel/water working pair. Renew. Energy 149, 1000–1017.
Vasta, S., Palomba, V., Frazzica, A., Costa, F., Freni, A., 2015. Dynamic simulation and performance analysis of solar cooling systems in Italy. Energy Procedia 81, 1171–1183.